

Effect of oxygen adsorption on the energy losses in grazing scattering of hydrogen ions on Ag(1 1 0)

J.E. Valdés^{a,*}, P. Vargas^a, L. Guillemot^{a,b}, V.A. Esaulov^b

^a Departamento de Física, Universidad Técnica Federico Santa María, Valparaíso, Casilla 110-V, Chile

^b Laboratoire des Collisions Atomiques et Moléculaires, (Unité Mixte de Recherche UMR 8625), bât 351, Université de Paris Sud, Orsay 91405, France

Available online 26 January 2007

Abstract

In this work we present a study of the effect of oxygen adsorption on the energy loss of 4 keV hydrogen ions, which are scattered off an Ag (1 1 0) single-crystal surface with varying coverages of oxygen. In this case oxygen adsorption leads to an added row reconstruction of the surface. We performed measurements for grazing angles as a function of crystal azimuthal orientation, which show large differences in energy losses. Experimental results are discussed in the light of trajectory calculations of protons scattered under grazing incidence conditions on the surface. Using non-linear models for stopping power, *ab initio* crystal structure calculations of the electronic density and semi-classical simulations, we obtain data that is in very good agreement with experimental results. These simulations in particular allow us to properly take into account the variations of the surface electronic density and hence obtain an accurate description of the energy loss processes for ion scattering along various azimuthal orientations of the target.

© 2006 Elsevier B.V. All rights reserved.

PACS: 34.50.Dy; 34.50.Bw; 61.85.+p

Keywords: Stopping power; Surface channeling; Ion scattering

1. Introduction

Over past years considerable effort has been made to understand the characteristics of the stopping of ions in matter [1–3]. In recent years a number of investigations have focussed on the question of energy losses undergone by ions scattered on surfaces [4–11]. Here the problem is rendered particularly complex, because regions above the first atomic layer of the surface, where the electronic density decreases, contribute to energy losses. Several attempts have been made to extract ion-surface distance dependent stopping powers and draw conclusions about stopping in an inhomogeneous electron gas [4–11]. A correct theoretical description of experimental data however requires a realistic description of the density corrugation above a crystal and particle trajectories.

In the present paper, we investigate the effect of adsorbing oxygen on energy losses of hydrogen ions scattered under grazing incidence on an Ag (1 1 0) surface for various crystalline directions. Oxygen adsorption on Ag(1 1 0) leads to an $n \times l$ added row reconstruction which at the highest – saturation-coverages corresponds to a $2 \times l$ structure (see e.g. [12,13] and Fig. 1(a)). In this case it has been shown that oxygen atoms are located between two adjacent silver atoms in an added row. This case thus presents the possibility of studying energy losses under well defined and different coverage conditions and different surface reconstructions.

In the following, we shall briefly outline the experimental approach and then present a modelling of the experimental results using computer simulations following an approach developed by us previously [14]. This approach allows us to study the differences induced by lattice steering effects in the energy loss distributions and most importantly *properly take into account the inhomogeneity of the surface electronic density*. We can thus obtain an accurate

* Corresponding author.

E-mail address: jorge.valdes@usm.cl (J.E. Valdés).

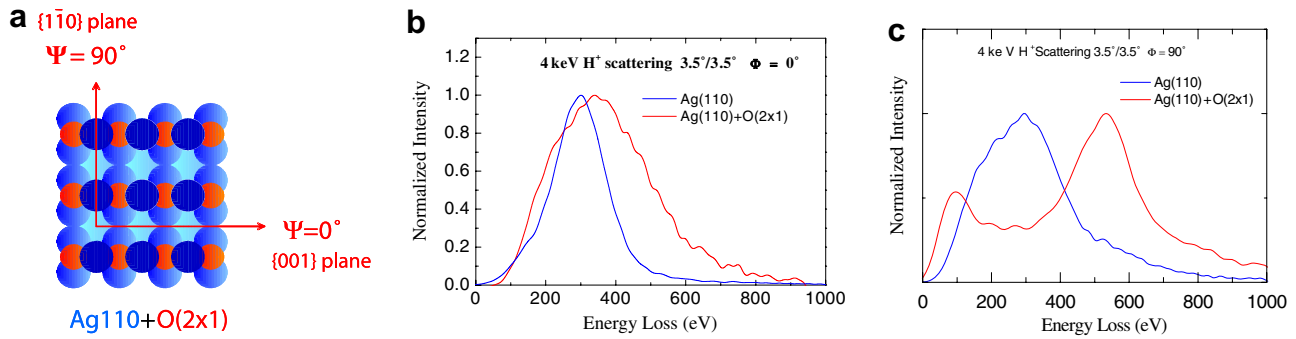


Fig. 1. (a) Schematic drawing of the oxygen covered Ag(110) surface for the 2×1 reconstruction. (c) General characteristics of energy loss spectra for H scattering on clean and oxygen covered Ag for the 0° (b) and 90° (c) directions.

description of the energy loss processes for ion scattering along various azimuthal orientations of the target.

2. Experimental results

A detailed description of the apparatus and the experimental procedure used for the present measurements is given elsewhere [15].

The crystal azimuthal setting is determined by measuring the scattered intensity of the ion beam in the forward direction during an azimuthal scan. This allows a precision better than 0.2° . In this paper we report results for grazing scattering for a total scattering angle of 7° for specular scattering conditions. The incident and exit angles to angle to the surface are of 3.5° set with an accuracy of about 0.1° . The acceptance angle of the detector in the scattering plane is 0.2° .

Fig. 1 present results of our measurements for incident 4 keV protons and scattered off as atoms in the main azimuthal directions, 0° and 90° in a Ag(110) clean surface and a Ag(110) + O(2×1) reconstructed surface. All the distributions present structures. One of the main features is the splitting of the main peak at 90° (clean silver) into two peaks for the Ag(110) + O(2×1) surface. Oxygen adsorption leads to a strong change in the structure of the energy loss spectra which broaden and in some cases develop a double peak structure, with a very large energy loss component. The spectra for other charge states (H^+/H^-) were similar.

3. Energy loss model and simulations

In order to understand the main features of the ion energy loss spectra obtained from grazing scattering we have developed a simulation code. In this section we briefly describe the main ingredients that we use in our code. More details may be found in our earlier papers.

3.1. Surface and bulk electron density

In order to describe the electronic density of surface and bulk in real space retaining their inhomogeneities, we have

performed detailed calculations of the Ag (110) system. Our description is based on the ab initio LMTO (linear muffin-tin orbitals) method which has been explained elsewhere [16,17]. The method is based on DFT (density functional theory) within the LDA (Local density approximation) for the exchange correlation potential. The calculation solves iteratively the Kohn–Sham equations taking into account the spatial environment of the atoms until self consistency is reached. The charge densities using this method are in excellent agreement with those obtained from a linear augmented plane-wave full-potential (LAPW) calculations, although LMTO uses an atomic sphere approximation for the one electron potential and empty spheres to simulate the interstitial region in open structures [17]. In Fig. 2 we show the planar average (XY) of the electron density as a function of depth Z , for Ag (110) and Ag(110) + O(2×1). On the average a decrease of the electron density at the surface is observed, due to the presence of the added row (2×1) of silver and oxygen.

The valence charge density was used to calculate the electronic stopping of the projectile along its trajectory. As we know the electronic charge density of the surface strongly depends on the azimuthal angle, so the electronic stopping will also depend on the relative orientation of the surface with respect to the ion azimuthal incidence. It is also clear that information on ion surface distance dependent stopping obtained from scattering experiments assuming an averaged electron density at any given distance from the surface would (see e.g. [4–11]) be unrealistic.

3.2. Simulations

The simulation of particle trajectories is made by solving the Newton equation of motion using the Runge–Kutta method. We use the Lenz–Jensen ion–atom interaction potential to describe the inter-atomic forces between the projectile and the lattice atoms, which is given by V_{lattice} . The equation that describes the ion trajectory is

$$\begin{aligned} \vec{F}(\vec{r}) &= M \frac{d^2 \vec{r}}{dt^2} \\ &= -\nabla V_{\text{lattice}}(\vec{r}, \vec{R}) - \nabla V_{\text{imag}}(z) + \vec{f}(\vec{v}, n(\vec{r})). \end{aligned} \quad (1)$$

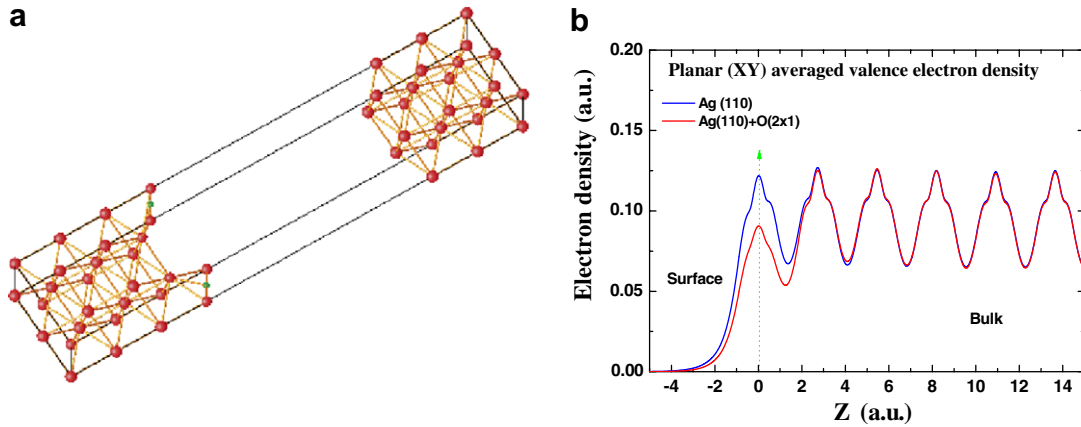


Fig. 2. (a) Super cell used in the LMTO calculation (b) Planar average (XY) of the electron density as a function of depth Z , for Ag (110) and Ag(110) + O(2 × 1).

In this equation, M is the projectile mass; r is the ion position and R the crystal atom position. The term $\vec{f}(\vec{v}, n(\vec{r}))$ corresponds to the friction force in the ion-electron interaction and depends locally on the electron density $n(\vec{r})$. In the integration of Newton equations, in each time step we consider the LDA, independently of the size of the electron gradient. Here we consider only the valence electron density contribution for this calculation. This consideration is valid for low ion velocities ($v \ll 1$ a.u.). Consideration of core electrons does not affect the final result, because the projectile does not probe small or intermediate impact parameters as we tested. The features of this friction force are described below. Also in the equation appears the image potential, which is necessary to consider in ion scattering trajectories. This force is time independent and is given in the approximation of Jones–Jennings–Jepsen (JJJ) for the surface barrier in a metal [18,19]. As mentioned above we also include the effect of lattice vibrations. The uncorrelated lattice vibrations are introduced assuming that the atoms are allowed to move independently of each other in all directions. Here we use the 1D-rms vibrational amplitudes obtained experimentally by Busch and Gustafsson [20] at room temperature, whose values are $u_x = 0.15 \text{ \AA}$, $u_y = 0.22 \text{ \AA}$ and $u_z = 0.16 \text{ \AA}$ for the first layer and $u_x = 0.11 \text{ \AA}$, $u_y = 0.15 \text{ \AA}$ and $u_z = 0.16 \text{ \AA}$ for the second layer. For the third and next layers we use the bulk value given by the tabulated Debye temperature equal to 225 K. In this calculation we use the standard Gaussian distribution for the probability of finding the atom at a distance u from its equilibrium position where we put a cut off in order to avoid large displacements that occur with low probability [21]. Inclusion of lattice vibrations in our calculations is just to consider a more realistic situation. Atomic vibrations produce effects in the multiple scattering, excluding or including some type of trajectories which reach the detector and hence affect to some extent the widths of the energy loss distributions.

The electronic energy loss is included explicitly in the dynamics of the particle using the instantaneous energy cal-

culated in a continuous slowing down process through a spatial static electron density. Actually, we mean a discrete slowing down process with a small time step of integration. Summation of these small amounts of energy transfer to the electrons will give the total energy loss of the projectile along its path. Also a spread of energy loss determined by the energy straggling effect is included. This important parameter is responsible for the shape of the energy loss spectra. The energy loss of particles in a homogeneous jellium, based on the non-linear or transport cross section model is given by [15],

$$\delta E(n) = nm_e v v_e \sigma_{tr}(n) \delta x. \quad (2)$$

In this equation δx is an infinitesimal displacement of the particle in each step of its motion along the trajectory, n is the local electron density, v the ion velocity, v_e is the electron velocity in the free electron gas model related to the electron density n through $v_e = (3\pi^2 n)^{1/3}$ and σ_{tr} is the transport cross section calculated quantum mechanically in terms of phase shifts $\delta_l(n)$. These are determined numerically by solving Schrödinger's equation for the scattering of electrons by a known screened potential or via DFT. This is a self-consistent model to adjust the screening constant and insure the Friedel sum rule is satisfied.

In a similar manner and using the same nonlinear model we include the quantum fluctuations in the energy loss, the energy loss straggling, given by [22]

$$\Omega^2(n) = 3nv^2 v_e^2 \delta x \int d\sigma(n, \theta) \sin^3(\theta/2), \quad (3)$$

here $d\sigma$ is the differential scattering cross section calculated also from the phase shifts $\delta_l(n)$.

3.3. Threshold effect

Several linear and non-linear theoretical calculations of the stopping power for slow ions predict a simple proportionality with the ion velocity [3] in the case of metallic targets. The origin of this velocity dependence can be traced

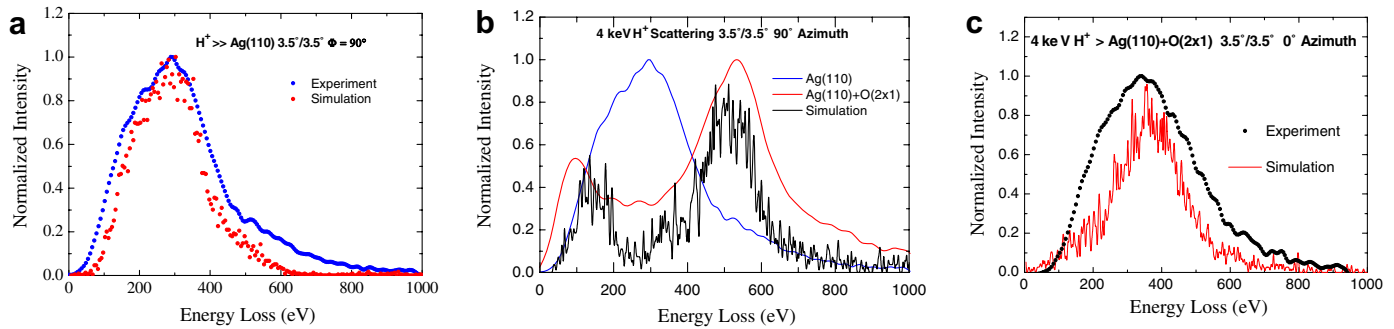


Fig. 3. Experimental and simulated energy loss spectra for the (a) 90° direction for clean Ag, (b) 90° direction for oxygen covered Ag and (c) 0° direction oxygen covered Ag. Incident ion energy is 4 keV.

back to the basic properties of the free electron gas model. However, recent experiments on energy loss of protons in metals like Cu, Ag, Au and Pd have shown significant deviations from this prediction [23,24], for ion energies below about 5 keV. This experimental behaviour was explained as arising from band structure effects in the excitation of d-electrons in those metals, where the electronic structure, represented through the density of electronic states, plays a fundamental role in the stopping curve behaviour as a function of velocity. Regarding this electron density, the corresponding electron states in the solid are localized and bound (according to the appropriate density of states), and so the creation of an electron-hole pair is achieved only if the particle loses a minimum of energy in a binary collision. This energy threshold is the difference between the Fermi energy and the energy of the electronic state of the involved electron. Then, only a fraction of the electrons at the instantaneous projectile position can be excited and contribute to the stopping power and energy loss straggling [24]. Summarizing, the energy loss and straggling are both a function of the particle velocity and of the local electron density.

Finally, with all of these ingredients we solve the Newton equation in each time step along the trajectory of the particle. With these calculations we can obtain the trajectories for each particle and the final position and velocity after the reflection of the particle from the surface.

4. Results

4.1. Simulations

The simulations were done for at least 500,000 trajectories. Using our program we can easily obtain trajectories, energy loss distributions and angular distributions. In particular we can obtain energy loss distributions for particles travelling above the surface or inside the solid, and analyse the contribution of these trajectories to the total energy loss spectrum. Here we shall show general results of energy loss distributions as a function of the azimuthal orientation of the target.

In the Fig. 3 we show a comparison between experimental and calculated energy loss distributions for 4 keV pro-

tons incident onto Ag(110) surface and Ag(110) + O(2 × 1) surface. At the left is the energy loss distribution for protons scattered in Ag(110), blue¹ points correspond to the experiment and red points correspond to the simulation using our code. At the right the figure shows the effect of the oxygen adsorption on silver for the same direction. Fig. 3(c) gives results for the 0° direction. The agreement between both, experiment and simulation is quite good in both cases.

The analysis of the various trajectories and associated energy losses allows us to understand the characteristics of the doubling of the energy loss spectrum for the 90° direction. The low energy peak is due to particles scattered on top of the atomic rows. The energy losses for scattering above the Ag and the O atoms of the added rows (see Fig. 1(a)) are quite similar. The peak at large losses is due to trajectories travelling between the second and third atomic layers. The structure at about 350 eV is due to particles travelling between the first and second atomic layers. The larger energy loss that one observes for the 0° direction as compared to the clean surface is due to the appearance of zig-zag trajectories for particles travelling between the added rows.

5. Conclusions

This paper presents a joint experimental and theoretical investigation of energy losses in hydrogen ion scattering on Ag(110). The experimental results are compared to calculations of particle energy losses, in which no arbitrary assumptions about the stopping in the electron selvedge of the metal are made. The electronic density of the solid is obtained through first principles calculations and is then used to determine the stopping force along the particle trajectory. We include a quantum dissipative friction force resulting from the interaction with the valence (s, p and d) electrons using a non-linear stopping model, which includes the so called “threshold effect” for the excitation of d electrons as described. We solve the Newton equation of the particle under the influence of the forces due to the

¹ For interpretation to the color in Figs. 1–3, the reader is referred to the web version of this article.

nuclei and core electrons and the force from the surface image potential model. Finally we include the effect of lattice vibrations.

This description allowed us to study the differences induced by lattice steering effects in the energy loss distributions. The results of these simulations agree very well with experiment. As opposed to approaches used in earlier works on surface scattering, these simulations in particular allow us to *properly take into account the variations of the surface electronic density* and hence obtain an accurate description of the energy loss processes for ion scattering along various azimuthal orientations of the target.

Some minor problems remain which could be related to some uncertainties in the knowledge of the exact charge state of the particles during scattering and possible existence of some steps. Solution of these relies on a refined analysis of the electron transfer processes which are not presently available.

Acknowledgement

This work was supported by the France-Argentina and France-Chile, ECOS-Conicet and ECOS-Conicyt collaboration projects (C02E07), FONDECYT grant # 1030175, internal grant USM-DGIP # 11.04.23 and Chilean Millennium Scientific Initiative under Contract No. P-02-054-F.

References

- [1] J. Lindhard, M. Scharffy, H.E. Schiott, K. Dans, Vidensk. Selsk. Mat. Fys. Medd. 33 (14) (1963).
- [2] D.S. Gemmell, Rev. Mod. Phys. 46 (1) (1974).
- [3] M.J. Puska, R.M. Nieminen, Phys. Rev. B 27 (1983) 6191; P.M. Echenique, R.M. Nieminen, R.H. Ritchie, Solid State Commun. 37 (1981) 779.
- [4] A. Garcia-Lekue, J.M. Pitarke, Phys. Rev. B 64 (2001) 35423; M. Alducin, V.M. Silkin, J.I. Juaristi, E.V. Chulkov, Phys. Rev. A 67 (2003) 032903; J.E. Miraglia, M.S. Gravielle, Phys. Rev. A 67 (2003) 062901.
- [5] A. Niehof, W. Heiland, Nucl. Inst. and Meth. B 48 (1990) 306; A. Nürmann, W. Heiland, R. Monreal, F. Flores, P.M. Echenique, Phys. Rev. B 44 (2003) 1991.
- [6] A. Robin, W. Heiland, J. Jensen, J. Juaristi, A. Arnau, Phys. Rev. A 64 (2001) 52901.
- [7] A. Robin, J. Jensen, D. Osterman, W. Heiland, Nucl. Inst. and Meth. B 193 (2002) 568.
- [8] K. Kimura, M. Hasegawa, M. Mannami, Phys. Rev. B 36 (1987) 7.
- [9] H. Winter, C. Auth, A. Mertens, A. Kirste, M.J. Steiner, Europhys. Lett. 41 (1998) 437; H. Winter, J.I. Juaristi, I. Nagy, A. Arnau, P.M. Echenique, Phys. Rev. B 67 (2003) 245401.
- [10] A. Arnau, P.M. Echenique, Phys. Scripta 677 (1993) T49.
- [11] L. Guillemot, E. Sanchez, V.A. Esaulov, Nucl. Inst. and Meth. B 212 (2003) 20.
- [12] M. Canepa, P. Cantini, L. Mattera, S. Terreni, F. Valdenazzi, Phys. Scripta 41 (1992) 226.
- [13] M. Canepa, P. Cantini, L. Mattera, E. Narducci, M. Salvietti, S. Terreni, Surf. Sci. 322 (1995) 271.
- [14] J.E. Valdés, P. Vargas, N.R. Arista, Phys. Rev. A 53 (1996) 1638.
- [15] V. Esaulov, L. Guillemot, O. Grizzi, M. Huels, S. Lacombe, Vu Ngoc Tuan, Rev. Sci. Inst. 67 (1996) 1.
- [16] O.K. Andersen, O. Jepsen, Phys. Rev. Lett. 53 (1984) 2551; O.K. Andersen, O. Jepsen, D. Gloetzel, in: F. Bassani, F. Fumi, M.P. Tosi (Eds.), Highlights of Condensed Matter Theory, North-Holland, New York, 1985; O.K. Andersen, O. Jepsen, M. Sob, in: M. Yussouff (Ed.), Lecture Notes in Physics: Electronic Band Structure and Its Applications, Springer-Verlag, Berlin, 1987.
- [17] O.K. Andersen, Z. Pawłowska, O. Jepsen, Phys. Rev. B 34 (1986) 5253.
- [18] O. Jones, P.J. Jennings, O. Jepsen, Phys. Rev. B 29 (1984) 6474.
- [19] N.V. Smith, C.T. Chen, M. Weinert, Phys. Rev. B 40 (1989) 7565.
- [20] B.W. Busch, T. Gustafsson, Surf. Sci. 407 (1998) 7.
- [21] M.T. Robinson, O.S. Oen, Phys. Rev. 132 (1963) 2385.
- [22] J.C. Ashley, A. Gras-Marti, P.M. Echenique, Phys. Rev. A 34 (1986) 2495.
- [23] R. Blume, W. Eckstein, H. Verbeek, Nucl. Instr. and Meth. 168 (1980) 57; R. Blume, W. Eckstein, H. Verbeek, Nucl. Instr. and Meth. 194 (1982) 67; R. Blume, Doctoral thesis, München, den 31 Juli 1980, private communication by W. Eckstein.
- [24] J.E. Valdés, G. Martínez, G.H. Lantschner, J.C. Eckardt, N.R. Arista, Nucl. Instr. and Meth. B 73 (1993) 313.